# Simulation of Space Charge Characteristics of Epoxy Materials at High Temperature

**Xingqiao Li, Kun Li, Shiyu Jin, Qianchuan Zhao, Ning Huang, Qianchuan Zhao, Honliang Zhang, and Hai Jin**

**Abstract** The main insulating material of converter transformer bushing is epoxy composite material, epoxy composite material has prominent interface effect and obvious space charge accumulation under high temperature, which is easy to cause electric field distortion and aging of insulation material, leading to bushing insulation failure. There is little research on numerical simulation of space charge of epoxy composites at high temperature, and the influence mechanism of space charge effect on casing electric field is not clear. In this paper, the space charge characteristics of epoxy composites are studied from the perspective of space charge. The simulation shows that the charge in the medium has different dynamic characteristics at different temperatures. High temperature conditions promote the injection and mobility of charges, making the extraction rate of holes less than the transport rate, and the migrated holes accumulate due to limited extraction, resulting in the accumulation of heterogeneous charges. The contribution of trapped carriers to space charge is most prominent during the later stage of pressurization. Due to the amass of different polarity charges, the electric field at the two electrodes is seriously distorted.

**Keyword** Epoxy · Bushing · Space charge · Carriers · Electric field distortion

## 1 Introduction

The converter bushing bears high voltage and large current carrying capacity during operation, and the temperature of central guide rod and capacitor core exceeds 100 °C [1]. When the insulation is subjected to high temperature, the space charge effect will become more prominent, causing electric field distortion, partial discharge and even breakdown, ultimately accelerating the aging of insulation materials, leading to insulation failure of bushings [2, 3]. Therefore, the properties of space charge in

X. Li · K. Li · S. Jin · Q. Zhao · N. Huang · Q. Zhao · H. Zhang (✉) · H. Jin
School of Electrical Engineering and Information Engineering, Lanzhou University of Technology, Lanzhou 730050, China
e-mail: zhanghl-518@qq.com



X. Dong and L. Cai (eds.), *The Proceedings of 2023 4th International Symposium on Insulation and Discharge Computation for Power Equipment (IDCOMPU2023)*, Lecture Notes in Electrical Engineering 1102, https://doi.org/10.1007/978-981-99-7405-4_61

insulation materials used for bushing at high temperature will provide a theoretical basis for insulation optimization, electric field analysis and many other aspects of the bushing.

In this study, we improve the bipolar carrier transport model and construct the finite element model of single-layer epoxy material in the software is constructed in COMSOL. Based on the course of carrier transport, capture, trapping, injection, and taking into account the limitation of carrier extraction, simulation analysis is carried out under high temperature conditions, and the space charge distribution and electric field distribution characteristics of epoxy materials at 40, 60, 80, 100 °C are obtained.

## 2 Bipolar Charge Transport Model Based on Limited Carrier Extraction

### *2.1 Brief Introduction of Physical Model*

To make the carrier transport part more obvious, some detailed physical processes are ignored and the following approximation is made:

(1) It is considered that the carrier transport in the medium is continuous and does not distinguish between crystalline and amorphous regions;
(2) Considering only a single trap level, it is considered that the influence of shallow traps is reflected in the change of carrier mobility;
(3) It is considered that the accumulation of heteropolar charges originates from electrode injection, and impurity ionization is not considered.

Based on the above approximation, Fig. 1 shows the physical model of bipolar carrier transport based on extraction restriction.

As shown in Fig. 1, When DC voltage is applied on both sides, holes and electrons are injected from the anode and cathode respectively, and some holes accumulate in the cathode and some electrons accumulate in the anode due to the limitation of carrier withdrawal. $S_{e\mu,ht}$ and $S_{et,h\mu}$ represent the recombination process of trapped charge (trapped electron/hole) and free charge (hole/free electron). Similarly, $S_{e\mu,h\mu}$ and $S_{et,ht}$ represent the recombination process between free charges and trapped charges of different polarity.

### *2.2 Mathematical Model*

The mathematical model of bipolar charge transport is mainly composed of the injection, extraction equation and transport equation of the electrode. For carrier injection, Schottky emission mode is adopted in this paper: when the applied field

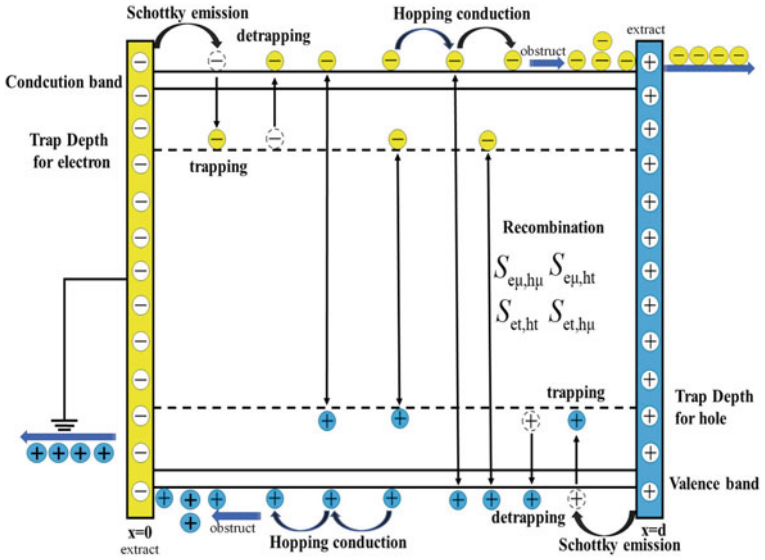


**Fig. 1** Physical model of bipolar charge transport based on carrier extraction constraints

strength is lower than 100 kV/mm, for the injection of electrons and holes on the surface of the cathode and anode [4], Schottky's law includes:

$$j_{\text{eihi}}(x,t) = AT(x)^2 \exp\left(\frac{-e\omega_{\text{eihi}}}{kT(x)}\right)\exp\left(\frac{e}{kT(x)}\sqrt{\frac{e|E(x,t)|}{4\pi\varepsilon_0\varepsilon_r}}\right) \tag{1}$$

In the above equation, T(0) and T(d) represent the temperature of the cathode and anode, $j_{ei}$ and $j_{hi}$ represent the injection current density of the cathode and anode, and w represents the injection barrier of holes and electrons at the interface; E(x, t) Is a random time electrode surface electric field; K is Boltzmann constant; Medium A is Richardson constant [5]. In order to prevent the non physical behavior when the electric field is 0 and the injection current is not 0, it can be obtained by modifying formula (1):

$$j_{\text{elhi}}(x,t) = AT(x)^2 \exp\left(\frac{-e\omega_{\text{eihi}}}{kT(x)}\right)\left[\exp\left(\frac{e}{kT(x)}\sqrt{\frac{e|E(x,t)|}{4\pi\varepsilon_0\varepsilon_r}}\right) - 1\right] \tag{2}$$

In this paper, in order to better express the withdrawing influence of electric field and temperature on carriers, the withdrawing process is defined in the same way as carrier injection $\omega_{eo}$ and $\omega_{ho}$ It represents the withdrawal barrier, and the carrier withdrawal limit is as follows [6]:

$$j_{\mathrm{eo/ho}}(x,t) = AT(x)^2 \exp\left(\frac{-e\omega_{\mathrm{eo/ho}}}{kT(x)}\right)\left[\exp\left(\frac{e}{kT(x)}\sqrt{\frac{e|E(x,t)|}{4\pi\varepsilon_0\varepsilon_{\mathrm{r}}}}\right) - 1\right] \quad (3)$$

The carrier transport in the epoxy composite can be described by the coupled PDE equations composed of current continuity (carrier convection reaction) equation, conduction equation and electrostatic field Poisson equation [7], which are expressed as follows:

$$\begin{cases} \frac{\partial n(x,t)}{\partial t} + \frac{\partial j(x,t)}{\partial x} = S_i(x,t) \\ j(x,t) = \mu(x,t)n(x,t)E(x,t) \\ \frac{\partial E(x,t)}{\partial x} = \frac{\rho(x,t)}{\varepsilon} \end{cases} \quad (4)$$

In the above equation, j is the current density in the medium; μ Is carrier mobility; $\rho$ Is the net charge density, which represents the sum of all carrier charges at time t and position x; Si is the source term, representing the interaction of different carriers; E is the electric field strength; $\varepsilon$ Is the relative dielectric constant. The convection term on the left side of the continuity equation represents the change of free charge caused by conduction current [8].

The carrier source term Si in formula (4) is specifically expressed as follows:

$$\begin{cases} S_{\mathrm{e}\mu} = -e \cdot S_{\mathrm{e}\,\mu,\mathrm{ht}} \cdot n_{\mathrm{e}\mu} \cdot n_{\mathrm{ht}} - B_{\mathrm{e}} \cdot n_{\mathrm{e}\mu} \cdot \left(1 - \frac{e \cdot n_{\mathrm{and}}}{N_{\mathrm{eot}}}\right) + D_{\mathrm{e}} \cdot n_{\mathrm{and}} \\ S_{\mathrm{and}} = -e \cdot S_{\mathrm{and,h}\,\mu} \cdot n_{\mathrm{and}} \cdot n_{\mathrm{h}\mu} - e \cdot S_{\mathrm{and,ht}} \cdot n_{\mathrm{and}} \cdot n_{\mathrm{ht}} + B_{\mathrm{e}} \cdot n_{\mathrm{e}\mu} \cdot \left(1 - \frac{e \cdot n_{\mathrm{and}}}{N_{\mathrm{eot}}}\right) \\ \quad -D_{\mathrm{e}} \cdot n_{\mathrm{and}} \\ S_{\mathrm{h}\mu} = -e \cdot S_{\mathrm{and,h}\,\mu} \cdot n_{\mathrm{and}} \cdot n_{\mathrm{h}\mu} - B_{\mathrm{h}} \cdot n_{\mathrm{h}\mu} \cdot \left(1 - \frac{e \cdot n_{\mathrm{ht}}}{N_{\mathrm{hot}}}\right) + D_{\mathrm{h}} \cdot n_{\mathrm{ht}} \\ S_{\mathrm{ht}} = -e \cdot S_{\mathrm{and,h}\,\mu} \cdot n_{\mathrm{and}} \cdot n_{\mathrm{h}\,\mu} - e \cdot S_{\mathrm{and,ht}} \cdot n_{\mathrm{and}} \cdot n_{\mathrm{ht}} - B_{\mathrm{h}} \cdot n_{\mathrm{h}\,\mu} \cdot \left(1 - \frac{e \cdot n_{\mathrm{ht}}}{N_{\mathrm{hot}}}\right) \\ \quad -D_{\mathrm{h}} \cdot n_{\mathrm{ht}} \end{cases} \quad (5)$$

where, $S_{\mathrm{e}\mu,\mathrm{ht}}$,$S_{\mathrm{et,h}\mu}$,$S_{\mathrm{et,ht}}$ Represent the recombination rate of free electron and trapped hole, trapped electron and free hole, trapped electron and trapped hole respectively; $B_e$ and $B_h$ represent the sinking coefficients of electrons and holes respectively; $N_{eot}$ and $N_{hot}$ represent the concentration of trapped electrons and trapped holes respectively; $D_e$ and $D_h$ represent the trapping rates of trapped electrons and trapped holes, respectively.

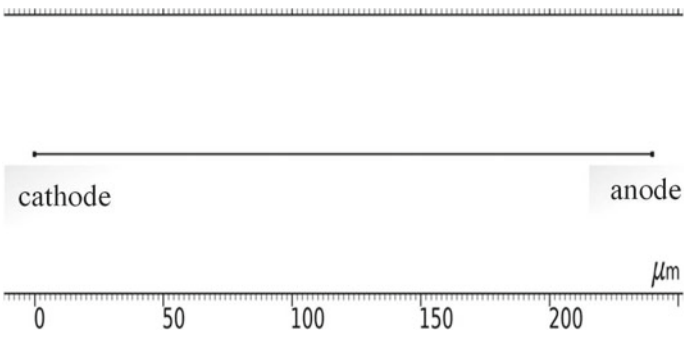


**Fig. 2** One-dimensional finite element model of epoxy sample

### *2.3 Finite Element Compression Model of Epoxy Material*

Figure 2 shows the one-dimensional geometric model of the epoxy flat sample in COMSOL.

The left end point is the cathode, and the right end point is the anode. The electrostatic field is coupled with the mass transfer field to simulate the charge transport process, and the transient charge density of four different carriers is calculated. Set the maximum unit length to 2.4 μm.

For macroscopic parameters such as electrode injection barrier and trap barrier, the measured data of our research group are combined. In order to reflect the influence of temperature and field strength on carrier mobility, jump conductance is used to describe the charge mobility [9] in the simulation, as shown in the following formula [8–11]:

$$\mu(x) = \exp\left(\frac{1.32 \times 10^{-5} \cdot |E| - 5715.5}{T}\right)/|E| \tag{6}$$

## 3 Simulation Results

### *3.1 Space Charge Distribution of Epoxy Materials at High Temperature*

The following external applied electric field 40 kV/mm is taken as an example for analysis. In order to clearly reflect the change trend of space charge within two hours of pressurization, the space charge nephogram corresponding to 40–100 °C is drawn in Fig. 3.

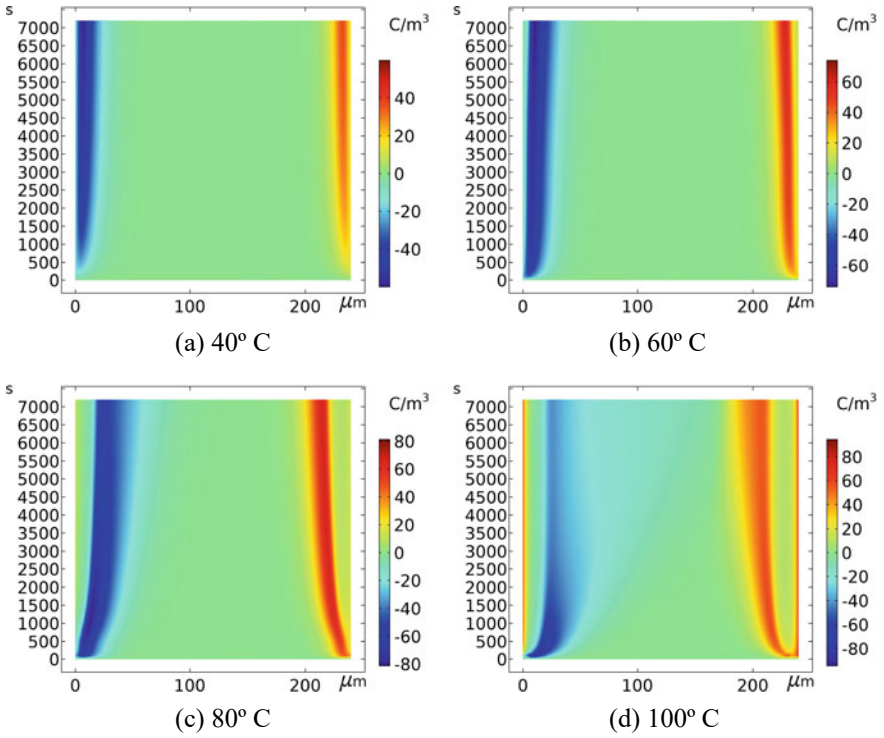


**Fig. 3** Cloud map of space charge distribution at different temperatures under 40 kV/mm electric field

It can be seen from Fig. 3 that at 40–60 °C, there is a homopolar charge distribution. In the first 100 s, the charge accumulation speed at 60 °C is significantly faster than that at 40 °C. When the temperature is 80 °C, starting from 1500 s, it is about 0–5 μm near the cathode There was a less obvious accumulation of positive charges at m, the maximum positive charge density was 10.3 C/m$^3$, and then the positive charges were covered by negative charges.0–8 μm near cathode at 100 °C There is always an accumulation of heteropolar charges at m, and the maximum positive charge density is 50.8 C/m$^3$. At this time, the negative charge diffusion depth of the cathode also increases significantly.

In order to study the charge distribution at different temperatures at the same time, Fig. 4 shows the space charge distribution at different temperatures at four times in 100–7200 s.

At 100s, the curve trends at four temperatures are roughly the same, and the charge peak gradually moves toward the interior of the medium. It can be seen that the space charge injection and diffusion at 40 °C are not obvious, and the area with space charge density of 0 is 60–100 μm. Taking the cathode as an example, the charge peaks at 40–100 °C are about 8 C/m$^3$, 35 C/m$^3$, 68 C/m$^3$and 95 C/m$^3$ respectively, indicating that the increase of temperature promotes the charge accumulation near

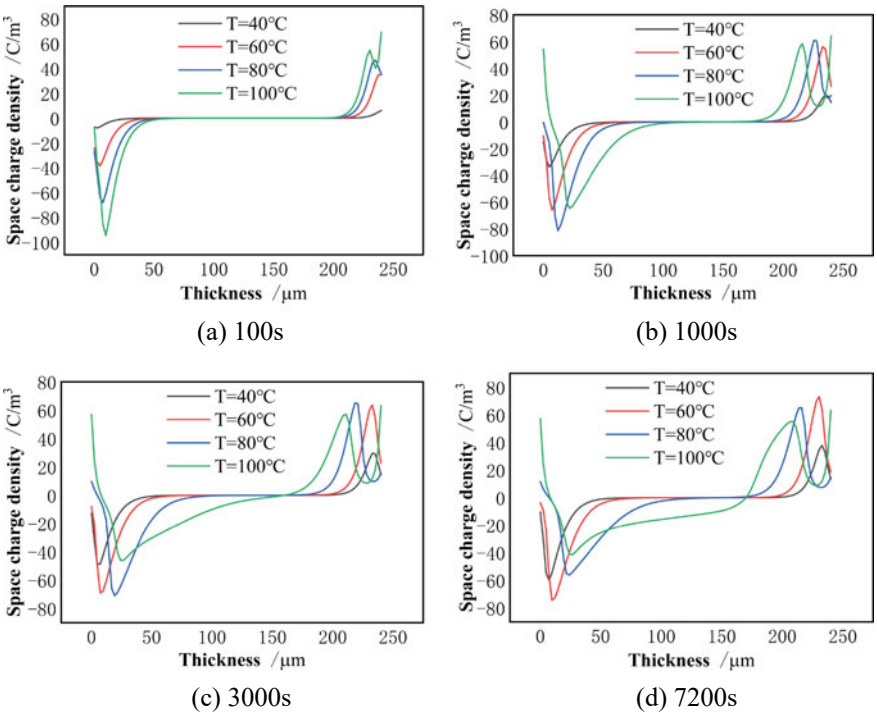


**Fig. 4** Space charge distribution at the same time and at different temperatures under 40 kV/mm electric field

the two electrodes. In addition, the charge accumulation near the anode is always less than the cathode at the early stage of pressurization.

To further understand the transport process of different carriers in the medium, Fig. 5 shows four carrier distributions at different times at 80 °C.

At 100 s, the injection of free holes/electrons is obvious, but the number of carriers transported to their opposite sides is limited. The cathode free electron injection barrier is small, although it is easy to inject, the capture rate is greater than the free hole, making the overall negative charge accumulation greater than the positive charge. At 1000–3000 s, it can be seen that the contribution of trapped carriers to space charge is the highest. Taking 3000 s as an example, the average density of trapped holes/trapped electrons accounts for 65.19% and 87.2% of the average positive/negative accumulated charge density respectively; 0–8 at 7200 μs. The concentration of trapped holes at m is greater than that of trapped electrons, and the superposition of the two makes the cathode present positive charge accumulation.

For the cathode, when the temperature is $\leq$ 60 °C, a large number of electrons are trapped near the cathode after injection, leading to the accumulation of negative charges. At the same time, the migrated holes accumulate due to limited extraction, and are compounded with negative charges. The accumulation amount near the

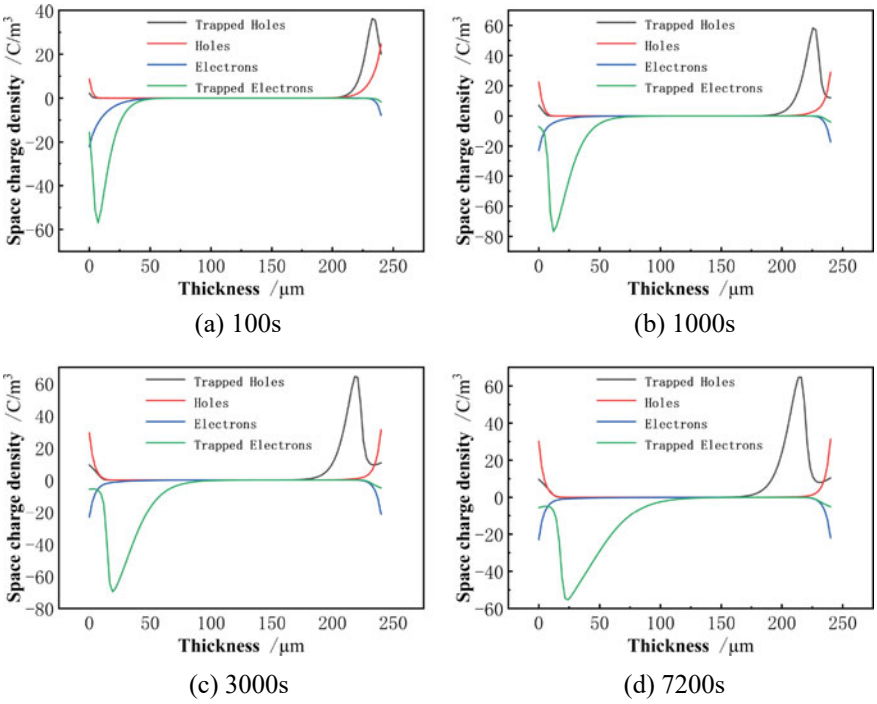


**Fig. 5** Carrier distribution at different times at 80 °C

interface is the largest, so the recombination amount is also the largest. Therefore, the charge density close to the cathode interface is smaller than the internal charge density. Then the temperature rise promotes the process of trapping and recombination, which leads to the increase of free charge density (the charge migrated in the shallow trap) and the acceleration of transport rate. When the temperature is $\geq$ 80 °C, because the hole extraction ability is weak, and the injected holes are continuously transported, the hole transport rate is greater than the extraction rate, and a large number of holes accumulate near the cathode to form an accumulation of heteropolar charges. The electron extraction rate near the anode is always greater than the transport rate, maintaining the accumulation of homopolar charges. The electron injection barrier is smaller than the hole, which leads to the injection electron density is greater than the hole, so that the overall electron accumulation is greater than the hole.

### 3.2 *Electric Field Distribution of Epoxy Materials at High Temperature*

The diffusion degree and accumulation density of the charge at different temperatures are different. The distribution of the charge determines the distribution of the electric field, which reacts on the distribution of the charge. The two depend on each other and together determine the transport process of the space charge. Eq. (7) is the electric field distribution corresponding to the space charge. Figure 6 shows the electric field distribution at different temperatures.

$$E(x) = \frac{1}{\varepsilon_0 \varepsilon_r} \int_{x_0}^{x} \rho(x) \mathrm{d}x \tag{7}$$

When the voltage is applied for 100 s, the electric field distribution trend at different temperatures is basically the same, that is, the electric field distortion near

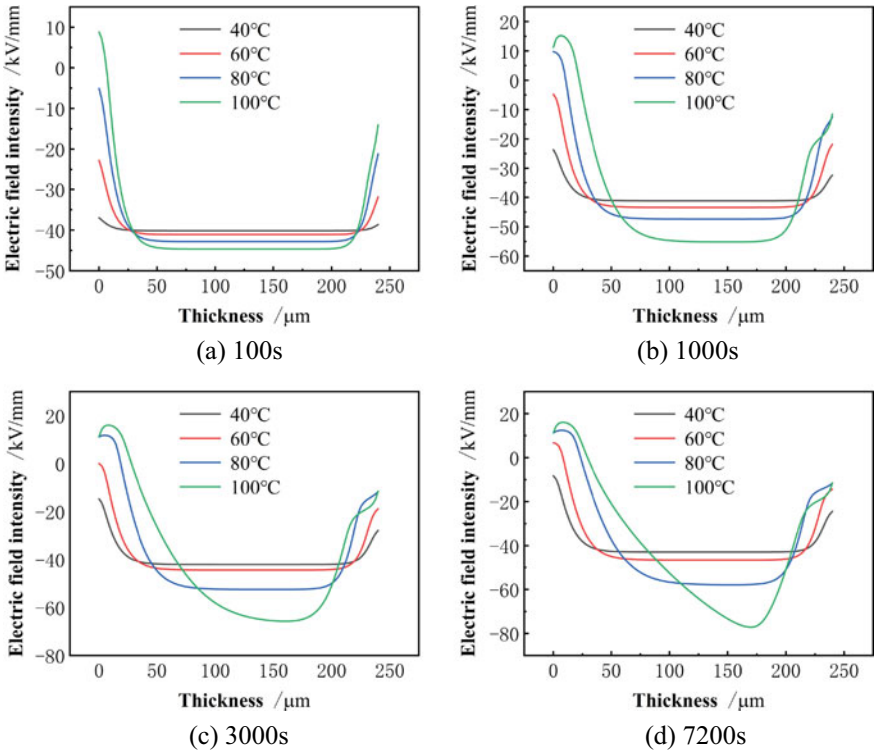


**Fig. 6** External applied electric field is 40 kV/mm and internal electric field distribution at different temperatures

the two poles is serious and the distortion degree near the cathode is greater than that near the anode. The electric field in the middle is relatively uniform, indicating that the space charge injection in the sample is not obvious at this time, and the reason for the asymmetric distribution near the two poles is that the negative charge accumulation near the cathode is greater than the positive charge accumulation near the anode. At 1000 s, the distribution of electric field is similar to that at 100 s. The difference is that with the increase of time, the distortion of electric field intensity in the middle is more obvious, indicating that more homopolar charges accumulate in the sample. At 100 °C, the electric field near the cathode shows a short curve of first increasing and then decreasing, which corresponds to the process of positive charges accumulating at the cathode and being covered by negative charges. The transient accumulation of heteropolar charges enhances the edge electric field.

When the pressure is 3000 s, the field strength in the middle of the 80–100°C curve rises significantly, and when the temperature is greater than 80 °C, the place of the maximum electric field moves to the right and is close to the anode, which indicates that the negative charge diffusion is further deepened. The electric field distribution at 7200 s is basically similar to that at 3000 s.

To more intuitively describe the distortion degree of temperature to electric field distribution, it can be expressed by defining distortion factor $C_d$, which is defined as follows:

$$C_d = \frac{|E_{max} - E_a|}{|E_a|}| \tag{8}$$

where, $E_{max}$ is the maximum electrical field in the model, and $E_a$ is the average electrical field of the voltage.

The electric field distortion factor at different temperatures is plotted according to Eq. (8) as shown in Fig. 7, which shows the electric field distribution at different temperatures. The degree of electric field distortion is measured by the distortion factor. The greater the distortion factor value, the greater the distortion degree of corresponding field intensity.

We can be obtained from Fig. 7 that the electric field distortion at temperature $\leq$ 60 °C is significantly less than that at temperature $\geq$ 80 °C. At 60 °C, the electric field distortion factor at the end of pressurization is only 0.15, while at 80 and 100 °C, the electric field distortion factors reach 0.41 and 0.92 respectively. According to the expression of Schottky injection and jump conductance, high temperature conditions promote the injection and mobility of charges, accelerate the carrier transport rate, lead to the accumulation of heteropolar charges, significantly increase the field strength near the cathode, and finally further increase the degree of electric field distortion.

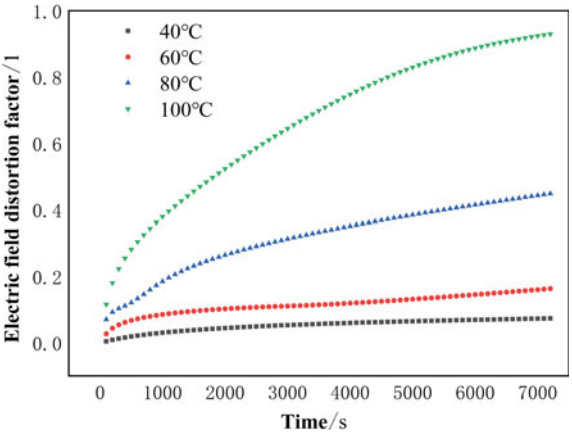


**Fig. 7** Electric field distortion factors at different temperatures when the applied electric field is 40 kV/mm

## 4 Conclusion

In this paper, based on the bipolar charge transport process, and considering the limitation of carrier extraction, the finite element model of epoxy material is constructed in COMSOL, and the space charge numerical simulation under extreme operating conditions is carried out. The electric field distribution features and space charge features of epoxy material under high temperature conditions are obtained. The main research work is summarized as follows:

(1) The finite element model of electrostatic field coupled with material transfer field is constructed, and the relevant model parameters are modified.
(2) It is found that the diffusion depth of positive and negative charges is increasing and the area with zero charge density is gradually shrinking under the long-term action and temperature rise. When the temperature of the cathode is $\leq 60$ °C, the charge density at the interface is less than the internal charge density, and when the temperature is $\geq 80$ °C, the heteropolar charge accumulation is formed near the cathode.
(3) The contribution of trapped carriers to space charge is the highest at the later stage of pressurization. The degree of electric field distortion at temperature $\leq 60$ °C is significantly less than that at temperature $\geq 80$ °C. This is because the high temperature conditions promote the increase of charge injection and mobility, which accelerates the carrier transport rate. However, carrier extraction is limited leads to the accumulation of heteropolar charges, which greatly increases the field strength near the cathode, and finally shows that the degree of electric field distortion is further aggravated. With the increase of temperature, the maximum electric field moves to the right, and the electric field distortion is obvious when the temperature is $\geq 80$ °C.

**Acknowledgements** This work is supported by the Gansu Provincial Science and Technology Commissioner Special Project (22CX8GA111) and Gansu Provincial Natural Science Foundation of China (21JR7RA237)

## References

1. Qang W, Liao J, Tian H et al (2017) Egularity analysis of the temperature distribution of epoxy impregnated paper converter transformer bushings. Dielectr Electr Insul IEEE Trans 24(5):3254–3264
2. Ruijin L, Jiyu W, Yuan Y et al (2016) Review on characteristics of new cellulose insulating paper under converter transformers. Trans China Electrotechnical Soc 31(10):1–15 (in Chinese)
3. Gong J, Li Z, Liu X (2016) Space charge characteristics of alumina/epoxy resin composites and AC electric field aging under high temperature and humidity. Trans China Electrotechnical Soc 31(18):191–198 (in Chinese)
4. Ma Z, Yang L, Bhutta MS et al (2020) Effect of thickness on the space charge behavior and dc breakdown strength of cross-linked polyethylene insulation. IEEE Access 8:85552–85566
5. Li L, Zhang X, Jin H et al (2021) Study on the temperature distribution of composite insulator of UHV-DC line considering solar radiation
6. Li K, Zhang H, Jin H et al (2021) Space charge dynamic characteristics of epoxy material under extreme conditions
7. Morab S, Sundaram MM, Pivrikas A (2022) Time-dependent charge carrier transport with hall effect in organic semiconductors for Langevin and Non-Langevin systems. Nanomaterials 12(24):4414
8. Shao Y, Tu Y, Chen G et al (2021) Simulation of space charge characteristics of epoxy resin under pulse voltage. In: 22nd International symposium on high voltage engineering (ISH 2021). IET, pp 1520–1525
9. Zhong X, Zheng Y, Dang B et al, Polarity effect of polymer space charge distribution under DC electric field. Chin J Electr Eng 36(24):6693–6701 + 6922 (1016) (in Chinese)
10. Tian F, Hou C (2018) A trap regulated space charge suppression model for LDPE based nanocomposites by simulation and experiment. IEEE Trans Dielectr Electr Insul 25(6):2169–2177
11. Zhang H (2019) Study on space charge characteristics of epoxy composites for UHV DC bushings under polarity reversal. Xi'an Jiaotong University (in Chinese)